The Effects of Atacticity, Comonomer Content, and Configurational Defects on the Equilibrium Melting Temperature of Monoclinic Isotactic Polypropylene

ERIC BRYAN BOND, JOSEPH E. SPRUIELL

Department of Material Science and Engineering, University of Tennessee, Knoxville, Tennessee 37996-2200

Received 18 September 2000; accepted 19 December 2000

ABSTRACT: A series of isotactic polypropylenes were investigated to account for total defect content using xylene fractionation and carbon-13 NMR experimental methods. The defects of interest were percent atactic content, copolymer content, and configurational defects. Experimental equilibrium melting temperatures were obtained for each material using the Gibbs-Thomson equation and extrapolation to infinite crystal thickness or the Hoffman-Weeks analysis. The experimental equilibrium melting temperature was then compared with the theoretical equilibrium melting temperature predicted by Flory's melting point depression model. Flory's model was found to fit the experimental data using an equilibrium melting temperature of 186°C when configurational defects are ignored. However, to account for all defects, the equilibrium melting temperature for 100% isotactic polypropylene must be increased from 186 to 192°C. © 2001 John Wiley & Sons, Inc. J Appl Polym Sci 81: 229–236, 2001

Key words: polypropylene; equilibrium melting temperature; atacticity; comonomer effect

INTRODUCTION

Isotactic polypropylene (iPP) is a polymer with unique morphological properties. Slight changes in tacticity, copolymerization, or elevated crystallization pressures can produce one or more of several types of crystal structures.[1–9] Therefore, the relationship of configurational chemistry, chemical species, and physical states interact to determine the stable phases and the thermodynamic properties of iPP.

An extensive amount of research has been done to understand the important molecular variables in iPP crystallization. Various authors[3,4,10–13] have used solvent fractionations to link the influence of molecular variables with crystallization kinetics (both bulk and crystal growth) and thermal properties such as melting temperature, crystallization temperature, and latent heat of fusion. Another body of studies[14–20] has used propylene blends to study the effects of diluent mixture on the various resin properties. Although these studies have been instrumental in understanding the effects of chemical microstructure on observable polymer properties, the effects have not been correlated with changes in iPP's equilibrium melting temperature.

The present study is intended to show how atactic content, configurational defects, and comonomer content affect the equilibrium melting temperature of α-iPP. The primary method used to determine the equilibrium melting temperatures of the resins was extrapolation using the Gibbs-Thompson equation and a combination of wide-angle X-ray diffraction (WAXD), small-

Correspondence to: J. E. Spruiell.
Contract grant sponsor: ExxonMobil Company.

Journal of Applied Polymer Science, Vol. 81, 229–236 (2001)

angle X-ray scattering (SAXS), and differential scanning calorimetry (DSC). Recently, we published an article detailing a WAXD/SAXS/DSC study of isothermally crystallized metallocene catalyzed iPP (miPP) resins.[21] The work showed the α-monoclinic equilibrium melting temperature was 186 ± 1°C, for the miPP resins in the study, as measured by this technique. In the present investigation, the same resins used in the earlier work will be studied further, along with three additional resins that differ in molecular weight, percent xylene solubles, comonomer content, and configurational defects.

THEORETICAL BACKGROUND

Flory and coworkers[22–33] developed the effects of atacticity, copolymerization, and configurational defects on the melting temperature from the theory of melting point depression. The change in melting point occurs due to a difference in chemical potential of the various chemical species in the system under consideration.

In general, the chemical potential of a substance J is defined as:

$$\mu_J = \left(\frac{\partial G}{\partial n_J}\right)_{p,T,n'} \quad (1)$$

where G is the Gibbs free energy, p is pressure, T is temperature, and n is the number of moles. The subscript n' signifies the amount of other components in the system. When equilibrium is present between the crystalline and liquid phases of the polymer, the chemical potential of the polymer repeat unit in the two phases must be equal $\mu_u^l = \mu_u^c$. This thermodynamic relationship defines the melting temperature (T_m) of the solid, which varies with the composition of both the liquid and solid phases. If a diluent is present in the liquid phase, T_m is the temperature at which the composition is a saturated solution. In a pure liquid polymer $\mu_u^l \equiv \mu_u^0$, where μ_u^0 is the chemical potential in the standard state of the pure liquid. At the equilibrium melting point (T_m^0) of the pure polymer, $\mu_u^0 = \mu_u^c$. In the presence of impurities or a diluent, μ_u^l will be less than μ_u^0. Thus, at the equilibrium melting temperature of the pure polymer, $\mu_u^l < \mu_u^c$. This necessitates a decrease in temperature to reestablish equilibrium $\mu_u^l = \mu_u^c$, after addition of the diluent. Thus, the decrease in equilibrium melting temperature, with addition of impurities, results from a change in free energy associated with the dilution of the pure liquid polymer at a given temperature and pressure.

The impurity/melting temperature depression relationship has been applied to situations were there is a noncrystallizable diluent (which can be a small molecule solvent or a polymer blend), polymer chain end groups and copolymerization. The present discussion concerns diluent and copolymerization effects. Configurational defects are treated in a similar manner as copolymerization, as explained below.

Diluent

For the case of a crystallizable liquid polymer containing a diluent at equilibrium with the crystalline polymer ($\mu_u^c - \mu_u^0 = \mu_u^l - \mu_u^0$), the effect of the diluent on the melting point is given by the Flory-Huggins expression[34–36]:

$$\frac{1}{T_m} - \frac{1}{T_m^0} = \frac{R}{\Delta H_u}\frac{V_u}{V_1}[(1 - v_2) - \chi_1(1 - v_2)^2], \quad (2)$$

where V is the molar volume of the chain repeat unit (subscript u) and diluent (subscript l), χ is the Flory-Huggins interaction parameter and v_2 is the volume fraction of the crystallizable polymer in the mixture, ΔH_u is the heat of fusion per repeat unit and T_m^0 is the equilibrium melting temperature of the pure homopolymer. Using the solubility parameter concept, χ can be obtained using[37–39]:

$$\chi = \frac{V_r}{RT}(\delta_1 - \delta_2)^2, \quad (3)$$

where δ_1 and δ_2 are the solubility parameters (square of the cohesive energy density) of the two components, and V_r is the reference volume. The solubility parameter concept is based on the theory of regular solutions, where there is no heat of mixing. If the two components form an ideal solution, or the diluent is present in small concentrations, eq (2) reduces to the copolymerization expression.

Copolymerization

In a copolymer consisting of A units which crystallize and B units that do not crystallize, with the two units occurring in random sequence along

Table I Resin Molecular Weight Characteristics

Sample Code	Catalyst	MFR[a]	Polydispersity	M_z (Kg/mol)	M_w (Kg/mol)	M_n (Kg/mol)
M10	Metallocene	10	2.65	454.7	256.4	96.8
M22	Metallocene	22	2.25	324.9	192.1	85.4
M32	Metallocene	32	2.28	287.4	172.5	75.6
ZN35	Ziegler-Natta	35	3.29	427.9	189.1	57.5
M100	Metallocene	100	2.27	219.0	123.6	54.5
ZNHT	Ziegler-Natta	36	2.22	—	131.1	59.0
ZN-5RCP	Ziegler-Natta	31	2.26	—	150.1	66.5

[a] g/10 min at 230°C.

the chain, the presence of B units depresses the melting point according to:

$$\frac{1}{T_m} - \frac{1}{T_m^0} = -\frac{R}{\Delta H_u} \ln X_A \tag{4}$$

where X_A is the mol fraction of A units in the random copolymer. Equation (4) holds only if the copolymer units are distributed at random along the polymer chains. If A and B units of a copolymer occur in separate sequences, the melting point depression will be less than predicted by eq. (4). If A and B units tend to alternate along the chain, the melting depression will be greater.

According to Flory's original description[33] of what is classified as a copolymer, vinyl polymers that posses asymmetric carbon atoms consist of mixtures of d and l structural units. A rigorous application would include iPP as a copolymer of meso and recemic diads.

EXPERIMENTAL

Materials

A total of seven resins, supplied by ExxonMobil Chemical Company, were used in this work. Three resins are Ziegler-Natta catalyzed isotactic resins (zniPP) and the other four are metallocene-catalyzed resins (miPP). One of the zniPP resins is randomly copolymerized with ethylene (ZN-5RCP) to give a nominal yield of 5% by weight, ethylene content.

The molecular weight characteristics of the resins are given in Table I. All the resins are high molecular weight, fairly narrow molecular weight distribution polymers.

Quiescent melting and crystallization temperatures, as measured by DSC, are shown for each material in Table II. The heating and cooling rates for each cycle are 20°C/min, with a hold time at 230°C for 5 min before the crystallization cycle to erase the sample's thermal history. Under these conditions the peak DSC melting temperature ranges from 134.6°C for the copolymer to 167.7°C for the ZNHT homopolymer.

Stereoregularity data for the materials are shown in Table III. Xylene solubles fractionation was done to quantify the volumetric amount of atactic material. Carbon-13 NMR was performed to analyze the configurational stereochemistry of xylene insoluble material and to accurately calculate the percent ethylene content. The earlier ar-

Table II Resin Thermal Properties as Measured by DSC[a]

	Melting Temperature (°C)		Crystallization Temperature (°C)		
Sample Code	Peak	Onset	Peak	Onset	Melting Enthalpy (J/g)
M10	149.0	140.8	104.1	109.1	80
M22	150.9	143.4	100.2	105.5	84
M32	150.6	143.2	100.2	105.7	84
ZN35	163.8	152.4	102.6	109.1	91
ZNHT	167.7	160.1	115.0	120.8	98
M100	147.1	140.1	103.6	108.4	81
ZN-5RCP	136.4	129.2	93.1	97.8	43

[a] Heating and cooling rates of 20°C/min.

Table III Stereoregularity Characteristics of the Resins

Sample Code	% Xylene Solubles	% (w/w) Ethylene	[meso]	Meso Run Length (Number of Monomers)	Defects per 10,000 Units			
					Regio	Stereo	Ethylene	Total
M10	0.60	—	0.9781	60	91	76	—	167
M22	0.36	—	0.9776	68	43	103	—	146
M32	0.35	—	0.9752	64	44	113	—	157
ZN35	3.62	—	0.9774	102	0	80	—	80
M45	0.41	—	0.9756	67	42	107	—	149
M70	0.48	—	0.9766	63	38	121	—	159
M100	1.33	—	0.9738	52	88	104	—	192
ZNHT	0.30	—	0.9840	200	0	50	—	50
ZN-5RCP	6.72	5.91	0.9827	13[a]	0	83	680	763

[a] Ignoring ethylene content would yield an average MRL of 121.

ticle[21] should be referred to for experimental conditions of xylene fractionation and cNMR procedure.

Determination of Equilibrium Melting Temperature

The value of T_m^0 for all six homopolymers was determined using SAXS, WAXD, and DSC measurements. WAXD was used to determine the percent crystalline fraction and DSC the melting temperature of each sample. SAXS was used to determine the long period, which was then multiplied by the WAXD percent crystallinity to yield the lamellae thickness. A plot of melting temperature vs. inverse lamella thickness was then constructed. An extrapolation to infinite crystal thickness was made to determine the T_m^0, as shown for ZN35 and ZNHT in Figure 1.

The copolymer's T_m^0 was determined using the Hoffman-Weeks method[40–42]: when performed properly, the Hoffman-Weeks method also gives a reliable value of T_m^0 for a material.

EXPERIMENTAL RESULTS

The molecular weight distributions for the resins in this study are narrow with all materials having a relatively high degree of polymerization, as shown in Table I. Resin M100 has the lowest degree of polymerization (M_n), with 1298 monomeric units. Therefore, the effects of chain ends can be neglected for these resins, as the maximum depression will be 0.4 K when considering chain ends as defects.[33]

The thermal properties of these materials are given in Table II. The Ziegler-Natta catalyzed homopolymer resins have the highest observed peak melting temperatures, with the miPP homopolymers having significantly lower melting temperatures. The copolymer (ZN-5RCP) has an even lower peak melting temperature than the miPP resins, by roughly 10 K. The melting enthalpy follows the same trend as melting temperature.

The value of T_m^0 for each resin is given in Table IV. ZNHT, M22, and M32 all have extrapolated T_m^0 values of 186 ± 1°C, while the other materials fall below 186°C. The copolymer has the lowest T_m^0 at 151 ± 1°C. One interesting finding is that ZN35 has the lowest T_m^0, of the homopolymers, despite having the second highest peak melting temperature.

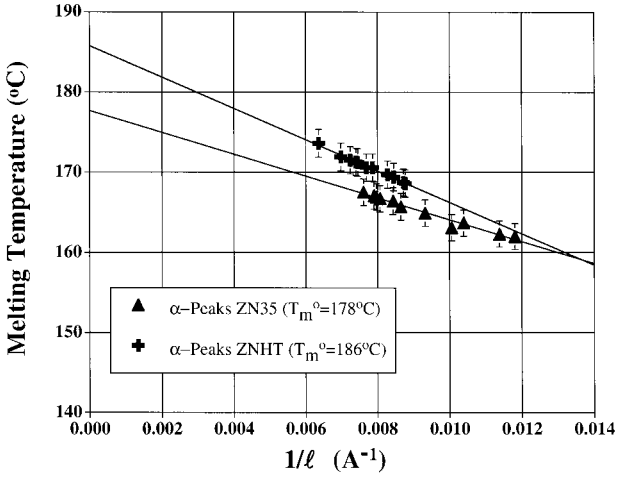

Figure 1 Equilibrium melting temperature of ZN35 and ZNHT determined by direct lamellae thickness measurements using SAXS, WAXD, and DSC.

Table IV Measured Equilibrium Melting Temperatures for the Resins

Sample Code	T_m^0 (°C)
M10	185 ± 1
M22	186 ± 1
M32	186 ± 1
ZN35	178 ± 1
ZNHT	186 ± 1
M100	183 ± 1
ZN-5RCP	151 ± 1

Stereoregularity and xylene solubles data are shown in Table III. The xylene soluble fraction is composed of atactic polymer chains, which are polymer chains that do not crystallize. The cNMR data are the defect content values after xylene fractionation to remove the atactic material. The copolymer contains 5.91 wt % ethylene, of which 79% can be found in -PPPEPPP- sequences. The mol fraction of meso diads is very similar for all materials. The difference between the highest and lowest mole fraction of meso diads is roughly 1%. The average meso run length is computed from the number of defects per 10,000 monomeric units. The zniPP homopolymer and copolymer resins had the fewest configurational defects, which we define as stereo and regio insertion errors during polymerization. It is also worth noting that the miPP resins have stereo and regio defects, and that their total configurational defect level is twice that of the zniPP homopolymer resins.

DISCUSSION OF RESULTS

Xylene Insolubles

Atactic polypropylene (aPP) and iPP are soluble in all proportions under most experimental conditions in the liquid melt. Recent work[19] has determined that aPP has a value of $\delta = 15.14M$-$Pa^{0.5}$ and iPP has a value of $\delta = 15.11M$-$Pa^{0.5}$. When $|\Delta\delta| < 2$, solutions usually form. The solubility parameters for iPP and aPP are extremely close, which allows the use of an ideal solution for an aPP/iPP blend.[19,33] Therefore, we shall treat the xylene solubles fraction as a diluent and use eq (4) directly as the limiting form for the diluent relationship.

The mol fraction of diluent for each resin is calculated and tabulated in Table V.

Copolymerization

For the case of iPP copolymerized with PE, the assumption is made that PE units are preferentially rejected from the growth front under most crystallization conditions. The samples in this study were crystallized slowly at high crystallization temperatures, an environment that should reduce or prevent any defect incorporation into the crystal. This is not without fault[43–47]; experimental results have shown that at high cooling rates or under quench conditions some defect inclusion can occur due to kinetic effects.

The mol percent ethylene content for the copolymer is given in Table V.

Configurational Defects

Isotactic polypropylene can be treated as a copolymer consisting of meso and racemic diads.[4,33] Defects found (ignoring branching) in zniPP resins are stereo, while miPP resins have both regio and stereo defects. There has been no direct experimental evidence to show rejection of configurational defects during the crystallization process in iPP. However, it seems most probable based on the knowledge that configurational defects disrupt the helical structure of an iPP chain. Regio defects would seem to be even more disruptive to the helix, due to severe methyl group repulsion. We proposed in an earlier work[21] that rejection of configurational defects into the fold surface region caused an increase in fold surface energy.

The mol percent of configurational defects is given in Table V.

Calculation of Equilibrium Melting Temperature

The mol fraction of crystallizable units is defined as X_A and noncrystallizable units X_B. X_B is the total mol fraction noncrystallizable units, combin-

Table V Mol Fraction of Substituent Defects

	X_B (mol Fraction Defects)		
Sample Code	Diluent	Copolymer	Configurational
M10	0.0060	0	0.0219
M22	0.0036	0	0.0224
M32	0.0035	0	0.0248
ZN35	0.0362	0	0.0226
ZNHT	0.0030	0	0.0160
M100	0.0133	0	0.0262
ZN-5RCP	0.0672	0.0733	0.0173

ing diluent, copolymer, and configurational defects for each resin:

$$X_B = X_{\text{diluent}} + X_{\text{copolymer}} + X_{\text{configurational}} \quad (5)$$

Using this approach, the equilibrium melting temperature was calculated for each resin using Flory's melting depression relationship. Figures 2 and 3 show a comparison of the calculated and experimental equilibrium melting temperatures, as a function of molar defect content. In Figure 2, only the diluent and copolymer effects were included; configurational defects are omitted from the calculation of X_B. Figure 3 includes all defects, diluent, copolymer content, and configurational defects. In each case, the solid line is the theoretical prediction using Flory's method with an assumed T_m^0 of 186°C for defect free α-iPP. The heat of fusion (ΔH_f) was assumed to be 167 J/g, based on experimental work done on these same samples.[21]

Flory noted that defect content less than 1 mol %, will not likely effect T_m^0 appreciably, due to the low ΔH_f found in most polymers.[33]

When considering only the diluent effect for each resin, the comparison between theory and experiment are close for the homopolymers. However, the theory does not accurately predict the copolymer melting value.

The effects of diluent and copolymer together are predicted accurately by the Flory theory, as shown in Figure 2. All data points fall on the theoretical prediction using the Flory model and T_m^0 of 186°C.

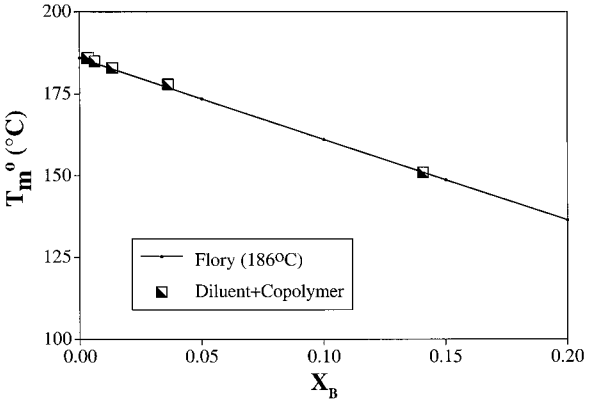

Figure 2 Calculated and experimental equilibrium melting temperature vs. mole fraction diluent and comonomer content. The solid line represents Flory's theoretical melting temperature using 186°C as the equilibrium melting temperature of defect free isotactic polypropylene (ignoring configurational defects).

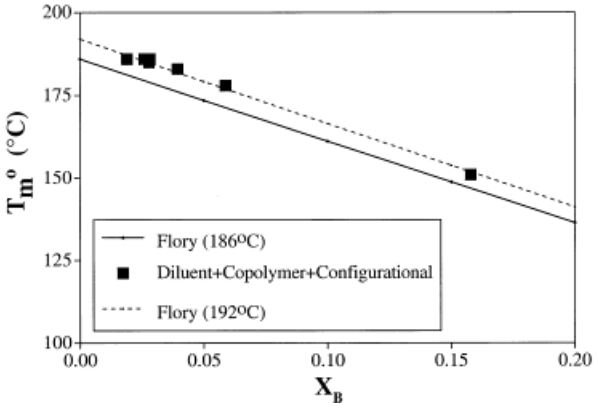

Figure 3 Calculated and experimental equilibrium melting temperature vs. the sum of mole fraction diluent, comonomer, and configurational content. The dotted line represents Flory's theoretical melting temperature using 192°C as the equilibrium melting temperature of defect free isotactic polypropylene.

The mol % ethylene has been modified from the original total of 5.91 wt %. This was necessary due to only 79% of the ethylene units being isolated among blocks of propylene units, i.e., random. The exact distribution is not known for all ethylene units; therefore, we split the difference and used an aggregate of 5.32% as the portion contributing to the *effective* random copolymer content.

When all defects (i.e., diluent, copolymer and configurational) are included in the molar defect fraction calculation, as shown in Figure 3, none of the experimental points lie on the Flory model line using a T_m^0 of 186°C for the pure, defect free polymer. Clearly, the theoretical prediction and experimental work disagree for these conditions. There are three possible reasons for the observed difference. (1) The value of ΔH_f used in the theoretical calculation is wrong; (2) the value of T_m^0 for the pure polymer used in the calculation is wrong; (3) another possible reason is that all previous researchers failed to account for configurational defects in their iPP resins.

We know that the value of ΔH_f is not the problem from experimental verification of ΔH_f on these resins.[21] Within experimental error, the value of ΔH_f is 167 J/g. The equilibrium melting temperature of a highly isotactic α-iPP has been quoted in the literature as having two different values, 186 and 210°C. Krigbaum,[48] Miller,[49] Campbell et al.,[50] and Bond et al.[21] report T_m^0

values of 186°C, while Fatou,[51] Monnassee,[52] and Fujiwara[53] report values near 210°C. Kamide and Yamaguchi[54,55] observed changes in melting temperature with crystallization time. The researchers observed that longer crystallization times lead to higher melting temperatures. This is now understood to be associated with lamellae thickening. Lamellae thickening increases as the crystallization temperature increases. Lamella thickening is the most likely explanation for the two T_m^0 values for highly isotactic α-iPP. Directly measuring the lamella thickness, as we have done, and making extrapolations to the T_m^0 will decrease the error found in making extrapolations from the crystallization temperature alone.

Only recently has stereoregularity information begun to appear with work associated with determining the T_m^0 of iPP resins. It is quite possible that most highly isotactic iPP resins studied in the past have roughly the same amount of configurational defects; therefore, all obtain similar T_m^0 values (by whatever method used).

A calculation using the mol % configurational defects for each resin, with the corresponding melting temperature for each resin gives a defect free T_m^0 for α-iPP of 192 ± 1°C, for each resin within experimental error. Using this new T_m^0 for defect free α-iPP, Figure 3 shows the new theoretical prediction using Flory's model, indicated by the broken line.

The new theoretical model accurately fits the experimental data when all defect types are included. This indicates that 192 ± 1°C is the proper, experimentally determined T_m^0 for a defect free, high molecular weight α-iPP homopolymer. This does imply that all previous experimental work is faulted; it suggests that previous investigators did not account for configurational defects that were present in all materials studied. These results further suggest that the T_m^0 for all iPP determined thus far are for samples containing substantial defect content.

CONCLUSIONS

Flory's theory of melting point depression has been used to analyze the influence of xylene insolubles, copolymer content, and configurational defects on the equilibrium melting temperature of α-iPP. The value of T_m^0 for 100% isotactic PP homopolymer was obtained by extrapolating the results for our experimental samples to this condition. It was concluded that previously reported values for the T_m^0 of α-iPP have generally not properly accounted for the influence of defects in the molecular configuration of the PP sample. We propose that when configurational defects are accounted for, the T_m^0 for the α-phase, as determined by the Gibbs-Thomson extrapolation, in 100% defect free iPP is 192 ± 1°C.

The authors wish to thank the ExxonMobil Chemical Company for supplying the resins used in research and for carrying out the molecular characterizations. We also thank them for support of this research and permission to publish it.

REFERENCES

1. Boor, J. Ziegler-Natta Catalysts and Polymerizations; Academic Press: New York, 1979.
2. Wolfgruber, C.; Zannoni, G.; Rigamonti, E.; Zambelli, A. Makromol Chem 1975, 176, 2765.
3. Paukkeri, R.; Vannen, T.; Lehtinen, A. Polymer 1993, 34, 2488.
4. Randall, J. Macromolecules 1997, 30, 803.
5. Mezghani, K.; Phillips, P. Polymer 1995, 36, 2407.
6. Mezghani, K.; Phillips, P. Polymer 1997, 38, 5725.
7. Turner-Jones, A.; Aizlewood, J.; Beckett, D. Makromol Chem 1964, 75, 134.
8. Turner-Jones, A. Polymer 1971, 12, 487.
9. Morrow, D.; Newman, B. J Appl Phys 1968, 39, 4944.
10. Martuscelli, E.; Pracella, M.; Crispino, L. Polymer 1983, 24, 693.
11. Martuscelli, E.; Avella, M.; Segre, A.; Rossi, E.; Drusco, G.; Galli, P.; Simonazzi, T. Polymer 1985, 26, 259.
12. Burfield, D.; Loi, P. J Appl Polym Sci 1990, 41, 1095.
13. Janimak, J.; Cheng, S.; Zhang, A.; Hsieh, E. Polymer 1992, 33, 729.
14. Avalos, F.; Lopez-Manchado, M.; Arroyo, M. Polymer 1996, 37, 5681.
15. Nandi, A.; Maiti, P. Polymer 1997, 38, 2171.
16. Feng, Y.; Hay, J. J Appl Polym Sci 1998, 68, 381.
17. Starke, J.; Michler, G.; Grellman, W.; Seidler, S.; Gahleitner, M.; Fiebig, J.; Nezbedova, E. Polymer 1998, 39, 75.
18. Yamaguchi, M.; Miyata, H.; Nitta, K. J Polym Sci Polym Phys 1997, 35, 953.
19. Maier, R.; Thomann, R.; Kressler, J.; Mulhaupt, R.; Rudolf, B. J Polym Sci Polym Phys 1997, 35, 1135.
20. Crist, B.; Hill, M. J Polym Sci Polym Phys 1997, 35, 2329.
21. Bond, E.; Spruiell, J.; Lin, J. S. J Polym Sci Polym Phys 1999, 37, 3050.
22. Flory, P. J Chem Phys 1947, 15, 684.
23. Evans, R.; Mighton, H.; Flory, P. J Chem Phys 1947, 15, 685.

24. Flory, P. J Chem Phys 1949, 17, 223.
25. Flory, P. Trans Faraday Soc 1955, 51, 848.
26. Flory, P.; Vrij, A. J Am Chem Soc 1963, 85, 3548.
27. Flory, P. J Polym Sci 1956, 21, 345.
28. Evans, R.; Mighton, H.; Flory, P. J Am Chem Soc 1950, 72, 2018.
29. Flory, P.; Mandelkern, L.; Hall, H. J Am Chem Soc 1951, 73, 2532.
30. Mandelkern, L.; Flory, P. J Am Chem Soc 1951, 73, 3206.
31. Flory, P.; Bedon, H.; Keefer, E. J Polym Sci 1958, 28, 151.
32. Mandelkern, L.; Quinn, F.; Flory, P. J Appl Phys 1954, 25, 830.
33. Flory, P. Principles of Polymer Chemistry; Cornell Press: New York, 1953.
34. Flory, P. J Chem Phys 1941, 9, 660.
35. Huggins, M. Ann NY Acad Sci 1942, 43, 1.
36. Huggins, M. J Phys Chem 1942, 46, 151.
37. Hildebrand, J.; Scott, R. The Solubility of Nonelectrolytes; Nostrand-Reinhold: New York, 1950.
38. Hildebrand, J.; Scott, R. Regular Solutions; Prentice-Hall: Englewood Cliffs, NJ, 1971.
39. Biros, J.; Zeman, L.; Patterson, D. Macromolecules 1971, 4, 30.
40. Hoffman, J.; Weeks, J. J Res Natl Bur Stds 1962, A66, 13.
41. Hoffman, J.; Weeks, J. J Chem Phys 1962, 37, 1723.
42. Hoffman, J.; Miller, R. Polymer 1997, 38, 3151.
43. Cole, E.; Holmes, D. J Polym Sci 1960, 4, 245.
44. Walter, E.; Reding, F. J Polym Sci 1956, 21, 561.
45. Eichon, R. J Polym Sci 1958, 31, 197.
46. Swan, P. J Polym Sci 1962, 56, 409.
47. Helfand, E.; Lauritzen, J. Macromolecules 1973, 6, 631.
48. Krigbaum, W.; Vermatsu, I. J Polym Sci Phys 1965, 3, 767.
49. Miller, R.; Sidney, E. J Polym Sci Phys 1982, 20, 2297.
50. Mezghani, K.; Campbell, R.; Phillips, P. Macromolecules 1994, 27, 997.
51. Fatou, J. Eur Polym J 1971, 7, 1057.
52. Monnasse, B.; Handin, J. Colloid Polym Sci 1985, 263, 822.
53. Fujiwara, Y. Colloid Polym Sci 1987, 265, 1027.
54. Kamide, K.; Yamaguchi, K. Makromol Chem 1972, 162, 219.
55. Kamide, K.; Yamaguchi, K. Makromol Chem 1972, 162, 205.